



REFERENCE

NIST
PUBLICATIONS

NIST TECHNICAL NOTE 1326



U.S. DEPARTMENT OF COMMERCE / National Institute of Standards and Technology

Theory and Measurements of Radiated Emissions Using a TEM Cell

G.H. Koepke
M.T. Ma
W.D. Bensema

QC
100
-45753
NO.1326
1989

Theory and Measurements of Radiated Emissions Using a TEM Cell

G.H. Koepke
M.T. Ma
W.D. Bensema

Electromagnetic Fields Division
Center for Electronics and Electrical Engineering
National Engineering Laboratory
National Institute of Standards and Technology
(formerly National Bureau of Standards)
Boulder, Colorado 80303-3328



U.S. DEPARTMENT OF COMMERCE, C. William Verity, Secretary
Ernest Ambler, Acting Under Secretary for Technology
NATIONAL INSTITUTE OF STANDARDS AND TECHNOLOGY, Raymond G. Kammer, Acting Director

Issued January 1989

National Institute of Standards and Technology Technical Note 1326
Natl. Inst. Stand. Technol., Tech. Note 1326, 40 pages (Jan. 1989)
CODEN:NTNOEF

U.S. GOVERNMENT PRINTING OFFICE
WASHINGTON: 1989

For sale by the Superintendent of Documents, U.S. Government Printing Office, Washington, DC 20402-9325

Contents

	Page
1. Introduction.....	1
2. Background.....	3
3. Mechanical Considerations.....	9
4. Electrical Measurements.....	16
5. Concluding Remarks.....	18
6. References.....	19

List of Figures

Figure	Page
1. An arbitrary current source inside one half of a TEM cell.....	21
2. The device under test (DUT) is modeled by three equivalent orthogonal electric and three equivalent orthogonal magnetic dipoles.....	21
3. The six required orientations of the DUT inside a TEM cell.....	22
4. A simple dielectric cube and trough for positioning the DUT inside the TEM cell. The DUT is mounted inside the cube.....	23
5. Two views of the dielectric positioner for use inside a TEM cell.....	24
6. The face and axis definitions of the cube at the initial position.....	25
7. The cube position at the second measurement step.....	25
8. (a) Schematic representation of the 2 slots in the back wall of the trough, "L" (left) and "R" (right). (b) The view along the trough axis showing the schematic of a lifting pawl within a slot. The three positions, initial (1), intermediate (2), and final (3) are shown for each of the pawls moving in slots "L" and "R".....	26
9. Cube rotation, from the initial to the second measurement step, caused by the three successively higher positions of both the "L" and "R" lifting pawl actuators. This is defined as an "A" rotation, which is 90°	27
10. Cube rotation, from the second to the third measurement positions, caused by the three successively higher positions of only the "R" actuator pawl. This is defined as a "B" rotation, which is 90° . The "L" actuator, and left slot are omitted for clarity.....	27

11.	Detail of one of the two slots cut in the cube wall to engage the "R" lifting pawl needed for single actuator rotators (type B) of the cube.....	28
12.	Cube positions for measurement step numbers four, five, and six.....	28
13.	Cross-sectional view of a TEM cell showing the two cable positions which occur as the cable rotates. Also shown are the approximate electric and magnetic field lines in the cell.....	29
14.	Radiated emissions testing measurement system.....	30
15.	A flow diagram of the measurement and analysis sequences.....	31

List of Tables

Table	Page
1. Required measurement positions of the DUT inside the TEM cell..	10
2. Sequence of measurement steps, cube position changes, rotation types, and actuator sequencing for a complete cycle...	14

Theory and Measurements of Radiated
Emissions Using a TEM Cell

Galen H. Koepke, Mark T. Ma, and William D. Bensema

National Institute of Standards and Technology
Electromagnetic Fields Division
Boulder, CO 80303

The transverse electromagnetic cell is widely used to evaluate the electromagnetic characteristics of electrically small devices. This paper reviews the theoretical basis for a technique to quantify the radiated emissions from any such device in the cell. The technique is well suited to an automated test system provided that the mechanical motions required can be controlled by a computer. The difficulties associated with these mechanical motions are discussed and possible solutions are proposed. The measurement technique is also expanded to include multiple-frequency sources in addition to single-frequency sources.

Key words: automation; electrically small radiator; emissions; measurements; TEM cell

1. Introduction

The transverse electromagnetic (TEM) cell is a device widely used for establishing a known electromagnetic field for susceptibility testing, probe and antenna calibrations, and other applications where a contained electromagnetic environment is desired. The measurement procedures and the merits and limitations of the TEM cell are well documented for these types of tests [1,2,3,4]. The TEM cell is also capable of capturing the signals radiated from a device under test (DUT), and provided that the criteria for

using the cell are followed these emissions may be quantified completely (total power and radiated power pattern) [5,6,7]. The cell is especially useful for devices that emit very low-level signals because it provides isolation from the ambient environment that may mask the signals radiated by the DUT.

The TEM cell is an enclosed coaxial structure and is used at frequencies where only the fundamental TEM mode may exist, as its name implies. The polarization of the TEM mode is fixed with respect to the cell geometry. This characteristic is very convenient for small dipole-antenna calibrations where the antenna can be carefully aligned with the well known electric-field vector [3]. However, for more complex DUTs where the response or radiation pattern is unknown, a single orientation gives incomplete information. Single orientation information may be useful for relative comparisons such as modifications for interference hardening or suppression of signal leakage from the device. However, to completely characterize the radiation from a device, six orientations with respect to the TEM field are required [5,6,7].

The National Institute of Standards and Technology (NIST) has developed and experimentally verified a technique for complete characterization of emissions from an unknown source using the TEM cell [5,6,7]. Section 2 of this paper briefly reviews the theoretical basis and the mathematical requirements of the technique. Section 3 examines the mechanical requirements for positioning the DUT in the TEM cell along with the problems associated with cables and defining the DUT. Section 4 discusses the electrical measurements and the instrumentation associated with both single-frequency and multiple-frequency measurements. The use of a computer system for automation of the measurements and analysis of the data is also mentioned. A short conclusion then follows.

2. Background

The electric and magnetic fields generated by an arbitrary current source located inside a waveguide will propagate along the guide both forward (+) and backward (-), as shown in figure 1. These electromagnetic fields may be expressed as a summation of electric and magnetic basis functions $\bar{E}_n^{(\pm)}$ and $\bar{H}_n^{(\pm)}$ describing the field structure of each mode that can exist within the guide. An expansion coefficient (amplitude) a_n or b_n is associated with each basis function as follows

$$\bar{E}^{(+)} = \sum a_n \bar{E}_n^{(+)}, \quad \bar{H}^{(+)} = \sum a_n \bar{H}_n^{(+)}, \quad (1a)$$

$$\bar{E}^{(-)} = \sum b_n \bar{E}_n^{(-)}, \quad \text{and} \quad \bar{H}^{(-)} = \sum b_n \bar{H}_n^{(-)}. \quad (1b)$$

These coefficients a_n and b_n may be calculated given a known current source, and the power at either port of the waveguide can then be determined. The calculation is immediately simplified by noting that the TEM cell is to be used with only the dominant TEM mode ($n = 0$), that the source must be electrically small to reside in the cell, and that this small source is placed at the center of the cell, $z = 0$ (figure 1). In reality, however, the current source for most emitters is unknown. The Lorentz reciprocity theorem for perfectly conducting waveguide walls can then be applied to relate the unknown current source represented by a combination of both electric-dipole moment (\bar{m}_e) and magnetic-dipole moment (\bar{m}_m) to the coefficients a_0 and b_0 [7,8],

$$a_0 = -\frac{1}{2} (\bar{m}_e + jk \bar{M}) \cdot \bar{e}_0 \quad (2a)$$

$$b_0 = -\frac{1}{2} (\bar{m}_e - jk \bar{M}) \cdot \bar{e}_0 \quad (2b)$$

where \bar{e}_0 is the normalized transverse vector electric field inside the TEM cell, $\bar{M} = \bar{m}_m \times \bar{z}$, \bar{z} is the unit vector along the longitudinal axis of the TEM cell, and k is the free-space wave number. Physically, \bar{e}_0 is the fundamental-mode field generated at $z = 0$ when a power level of 1 watt is supplied to the TEM cell. For a well-constructed rectangular TEM cell, the field component parallel to the flat center conductor (septum) near the center of the cell will be very small and a good approximation for \bar{e}_0 is given by

$$\bar{e}_0 \approx q \bar{y} \approx \left[\sqrt{Z_0 P} / b \right] \bar{y} = \left[\sqrt{50} / b \right] \bar{y}, \quad (2c)$$

where \bar{y} is the transverse unit vector perpendicular to the septum, Z_0 is the impedance of the TEM line at $z=0$ (50 ohms), P is the power supplied to the cell (1 watt), and b is the separation distance (meters) in the y direction from the septum to the outer wall of the cell. Thus, \bar{e}_0 is known for a given cell. The unknowns \bar{m}_e and \bar{m}_m in (2a) and (2b) are given by

$$\bar{m}_e = J \bar{d\ell}, \quad \bar{m}_m = J' \bar{ds}, \quad (2d)$$

where J is a normalized filament current, $\bar{d\ell}$ is the directed length vector of the short dipole, J' is the normalized loop current, and \bar{ds} is the vector

loop area. The units for \bar{m}_e are in ampere-meter normalized with respect to a unit current (or meter) and for \bar{m}_m are in ampere-meter-squared normalized with respect to a unit current (or meter-squared). Clearly then, the units for a_0 and b_0 are in volts.

The dot product of \bar{e}_0 and the source terms given in (2a) and (2b) describes the coupling mechanism into the TEM mode in the cell and also illustrates the reason the values of a_0 and b_0 are sensitive to the orientation of the source in the cell.

A device (source) consisting of an arbitrary number of small electric dipoles and small magnetic dipoles can be modeled, through the principle of superposition, by three equivalent small orthogonal electric dipoles and three equivalent small orthogonal magnetic dipoles, as shown in figure 2. From the analysis point of view, once the amplitude and relative phase of these equivalent dipoles are specified, the radiation pattern and total power radiated may be calculated [7]. When the source parameters are unknown, as in the case of emissions from an arbitrary device, the amplitudes (a_0 and b_0) of the fields generated by the source are readily measured at the output ports of the TEM cell. The problem then involves determining the equivalent source dipoles from measured data. The expressions of a_0 and b_0 in (2a) and (2b) to the dipole moments \bar{m}_e and \bar{M} suggest that a simple addition and subtraction of a_0 and b_0 will separate the contribution of the electric-dipole and magnetic-dipole moments. The powers detected at the output of the device performing the addition and subtraction (for example a 0° and 180° hybrid junction) are then given by

$$P_s = |a_0 + b_0|^2 = |\bar{m}_e \cdot \bar{e}_0|^2 \quad (3a)$$

for the sum power, and

$$P_d = |a_0 - b_0|^2 = k^2 |\bar{M} \cdot \bar{e}_0|^2 \quad (3b)$$

for the difference power. Thus, the sum power relates only to the electric-dipole moments and the difference power relates only to the magnetic-dipole moments. A glance at the relative amplitude of these measurements will indicate the source type (electric or magnetic or both).

The unknown dipole moments in (3a) and (3b) are, in general, composed of three orthogonal components each. To determine the amplitude and phase of each component requires a set of unique equations which can be solved simultaneously. The necessary equations are developed by a series of six orientations of the device within the TEM cell. The sum and difference powers and the relative phase between the sum and difference ports are measured at each of the six orientations. The phase angle measurement is required, as can be seen later, to develop the radiation pattern for a device composed of both electric and magnetic sources [7]. Phase measurements can be omitted when the device is composed of only electric or magnetic sources (but not both), or when the only quantity desired is the total power radiated. The details and derivations of the equations needed to calculate the source characteristics, including the treatment of the phase information, have been presented in [7].

The unknown dipole-moment amplitudes, m_{eh} and m_{mh} ($h = x, y, z$) and relative phases between the same kind, $\psi_{eh} - \psi_{eh'}$ and $\psi_{mh} - \psi_{mh'}$ ($h, h' = x, y, z; h \neq h'$) can be computed by the detected sum power P_{si} and difference power P_{di} at the i -th DUT orientation ($i = 1, 2, \dots, 6$) as follows [7],

$$m_{ex}^2 = (P_{s1} + P_{s2} - P_{s3} - P_{s4} + P_{s5} + P_{s6}) / (2q^2) \quad (4a)$$

$$m_{ey}^2 = (P_{s1} + P_{s2} + P_{s3} + P_{s4} - P_{s5} - P_{s6}) / (2q^2) \quad (4b)$$

$$m_{ez}^2 = (-P_{s1} - P_{s2} + P_{s3} + P_{s4} + P_{s5} + P_{s6}) / (2q^2) \quad (4c)$$

$$m_{mx}^2 = (P_{d1} + P_{d2} - P_{d3} - P_{d4} + P_{d5} + P_{d6}) / (2k^2 q^2) \quad (4d)$$

$$m_{my}^2 = (P_{d1} + P_{d2} + P_{d3} + P_{d4} - P_{d5} - P_{d6}) / (2k^2 q^2) \quad (4e)$$

$$m_{mz}^2 = (-P_{d1} - P_{d2} + P_{d3} + P_{d4} + P_{d5} + P_{d6}) / (2k^2 q^2) \quad (4f)$$

$$\psi_{ex} - \psi_{ey} = \cos^{-1}((P_{s1} - P_{s2}) / (2q^2 m_{ex} m_{ey})) \quad (4g)$$

$$\psi_{ey} - \psi_{ez} = \cos^{-1}((P_{s3} - P_{s4}) / (2q^2 m_{ey} m_{ez})) \quad (4h)$$

$$\psi_{ez} - \psi_{ex} = \cos^{-1}((P_{s5} - P_{s6}) / (2q^2 m_{ez} m_{ex})) \quad (4i)$$

$$\psi_{mx} - \psi_{my} = \cos^{-1}((P_{d2} - P_{d1}) / (2k^2 q^2 m_{mx} m_{my})) \quad (4j)$$

$$\psi_{my} - \psi_{mz} = \cos^{-1}((P_{d4} - P_{d3}) / (2k^2 q^2 m_{my} m_{mz})) \quad (4k)$$

$$\psi_{mz} - \psi_{mx} = \cos^{-1}((P_{d6} - P_{d5}) / (2k^2 q^2 m_{mz} m_{mx})) \quad (4l)$$

where q is the previously defined y component of \bar{e}_0 [eq.(2c)]. The corresponding free-space radiation pattern of this emitter, in spherical coordinates referenced to the emitter center, can be expressed as

$$\begin{aligned}
P(\theta, \phi) = & \frac{15\pi}{r^2 \lambda^2} \left[(m_{ex}^2 + k^2 m_{mx}^2) (\cos^2 \theta \cos^2 \phi + \sin^2 \phi) \right. \\
& + (m_{ey}^2 + k^2 m_{my}^2) (\cos^2 \theta \sin^2 \phi + \cos^2 \phi) + (m_{ez}^2 + k^2 m_{mz}^2) \sin^2 \theta \\
& - 2\{m_{ex} m_{ey} \cos(\psi_{ex} - \psi_{ey}) + k^2 m_{mx} m_{my} \cos(\psi_{mx} - \psi_{my})\} \sin^2 \theta \sin \phi \cos \phi \\
& - 2\{m_{ey} m_{ez} \cos(\psi_{ey} - \psi_{ez}) + k^2 m_{my} m_{mz} \cos(\psi_{my} - \psi_{mz})\} \sin \theta \cos \theta \sin \phi \\
& - 2\{m_{ez} m_{ex} \cos(\psi_{ez} - \psi_{ex}) + k^2 m_{mz} m_{mx} \cos(\psi_{mz} - \psi_{mx})\} \sin \theta \cos \theta \cos \phi \\
& + 2k\{m_{ex} m_{my} \sin(\psi_{ex} - \psi_{my}) - m_{ey} m_{mx} \sin(\psi_{ey} - \psi_{mx})\} \cos \theta \\
& + 2k\{m_{ey} m_{mz} \sin(\psi_{ey} - \psi_{mz}) - m_{ez} m_{my} \sin(\psi_{ez} - \psi_{my})\} \sin \theta \cos \phi \\
& \left. + 2k\{m_{ez} m_{mx} \sin(\psi_{ez} - \psi_{mx}) - m_{ex} m_{mz} \sin(\psi_{ex} - \psi_{mz})\} \sin \theta \sin \phi \right] \quad (5)
\end{aligned}$$

where the relative phases between the different kind of dipole moments, $\psi_{eh} - \psi_{mh}$, can be computed by P_{si} , P_{di} and the detected relative phase (ϕ_i , $i=1,2,\dots,6$) between the two output ports [7]. One of them is specifically shown below:

$$\begin{aligned} \psi_{ex} - \psi_{my} = \phi_1 + \tan^{-1} \left[\frac{m_{ey} \sin(\psi_{ex} - \psi_{ey})}{m_{ex} + m_{ey} \cos(\psi_{ex} - \psi_{ey})} \right] \\ - \tan^{-1} \left[\frac{m_{mx} \cos(\psi_{mx} - \psi_{my}) - m_{my}}{m_{mx} \sin(\psi_{mx} - \psi_{my})} \right]. \end{aligned} \quad (6)$$

The total power radiated can be obtained by

$$\begin{aligned} P_t &= \int_{4\pi} P(\theta, \phi) d\Omega \\ &= \frac{40\pi^2}{\lambda^2} \left[m_{ex}^2 + m_{ey}^2 + m_{ez}^2 + k^2 (m_{mx}^2 + m_{my}^2 + m_{mz}^2) \right] \end{aligned} \quad (7)$$

The above equations show that the relative phase information ϕ_i is not needed if the unknown emitter is believed to be composed of one kind of dipole moments only (either \bar{m}_e or \bar{m}_m) or if the detailed radiation pattern given in (5) is not required.

3. Mechanical Considerations

A systematic procedure has been developed [5,6,7] using the rectangular Cartesian coordinates and six DUT orientations to satisfy the need as outlined in section 2. The details of the positioning are illustrated in figure 3 and the six required positions are listed in table 1. The

coordinates (x', y', z') are defined with respect to the DUT. The TEM cell coordinates (x, y, z) are fixed with respect to the cell with z along the length and x and y defining the transverse plane or cross section of the cell. The y coordinate is perpendicular to the flat septum and x is parallel to the septum. The cell coordinate system has its origin at the geometric center of the TEM cell and the DUT is placed at $(0, y_0, 0)$ (see figure 3). The coordinates of the DUT are aligned with the appropriate TEM cell axes. This preliminary alignment as shown in figure 3 is then followed by two successive rotations about the z axis (longitudinal) of the TEM cell. The resulting positions are summarized in table 1.

Table 1. Required measurement positions of the DUT inside the TEM cell

POSITION	Align DUT to cell axes then ROTATE about z	
1	$x' \rightarrow x, y' \rightarrow y, z' \rightarrow z$	45 degrees
2	" " "	135 "
3	$y' \rightarrow x, z' \rightarrow y, x' \rightarrow z$	45 "
4	" " "	135 "
5	$z' \rightarrow x, x' \rightarrow y, y' \rightarrow z$	45 "
6	" " "	135 "

An appropriate rotatable mechanism for mounting the DUT inside the TEM cell half-chamber must be fabricated. This mechanism may be as simple as the 90-degree non-metallic trough and cube shown in figure 4 where the DUT is placed inside the cube and the trough holds the cube at the correct position. This requires manual positioning at each of the six required positions but is simple, accurate, and inexpensive.

A more sophisticated approach has been prototyped that allows for automation of the mechanical rotation process using a similar cube for mounting the device and a 90-degree trough with pawls that lift and turn the cube in the trough. The measurement positions as defined in table 1 are unchanged but the sequence of attaining each position has been tailored (1,2,5,6,3,4, and return to 1) in order to minimize the mechanical movements required of the rotator system and to avoid twisting cables which may be parts of a DUT. The following description will refer to this sequence of positioning as measurement steps and the actual orientation of the DUT in a particular step as a measurement position using the definitions of table 1.

Design of a mechanical rotator for the DUT in a TEM cell is limited by several constraints:

1. Construction must be of dielectric (non-metallic) material.
2. Mass of the dielectric material must be kept to a minimum.
3. Positioning to each of the six positions must be accurate and repeatable, independent of the mass distribution of the DUT.
4. Any power or data cables must not be allowed to tangle or twist.
5. Ideally, power or data cables should be maintained in a constant configuration throughout the rotations.
6. The mechanism must be reliable. To this end the number of actuators should be kept to a minimum. Two or three is ideal.
7. Finally, feedback to a controlling computer should be available to tell the computer that each test position has been successfully

reached. Once the metal walled TEM cell is closed, visual feedback is eliminated.

The mechanical system described here satisfies all these conditions. A working prototype has been constructed that provided for all the above points except number 7, and a suggested approach to accomplish that will be described. The physical dimensions of the hardware are not specified. These dimensions will be determined by the physical size of the TEM cell and the devices placed in the cube. The center of the DUT should rotate about the point midway between the septum and outer wall of the TEM cell.

The positioner consists of a dielectric cube, containing the DUT mounted firmly inside and resting in a 90-degree dielectric trough that has convex end plates (figure 5). Flat end plates were used in the prototype and worked satisfactorily; slightly convex end plates would improve reliability.

To progress from one measurement step to the next, a 90-degree rotation of the cube about an axis projecting perpendicularly from a cube face is performed. Axis definition is most easily defined as projecting from three adjacent cube faces as shown in figure 6. The corner common to these three faces is labeled "C", and is delineated in all appropriate figures by a closed triangular mark. The axis definitions are not reproduced on the remaining figures.

The first change of position (position 1 to 2) is a 90-degree rotation of the cube about the z axis producing the orientation shown in figure 7. Motion is accomplished by force from two actuators that each moves a single pawl upward in a slot on the back face of the trough. The slots are labeled "L" (left) and "R" (right), and are shown schematically in figure 8(a). The actuators and attached pawl can be controlled individually. Figure 8(b) shows the sequence of motion performed by either actuator/pawl combination.

The cube is rotated by the upward motion of the pawl/actuator mechanism. The view down the z axis is shown in figure 9, for three successive locations of both "L" and "R" pawls. After the cube reaches the approximate position shown in figure 9(c), gravity causes the cube to fall to the bottom of the trough. The sides of the trough and end walls are covered with a low friction material such as fluorocarbon to facilitate this settling action. Because the sides of the trough are constructed to allow for just the width of the cube, the cube is automatically centered as it settles to the bottom of the trough. This type of axis rotation is arbitrarily defined as an "A" rotation. At the completion of the A rotation, the actuators are returned to their starting position. On the trip down, the pawls rotate out of the way of the cube.

The system is now ready to begin the transition to the third measurement step (position 5), a maneuver defined as a "B" rotation. This is accomplished by raising only one actuator, in this case the "R" actuator. The motion produced is shown in figure 10. When the cube reaches the position shown in figure 10(c), gravity causes the cube to slip until face y' contacts the right-hand end wall, and the cube falls into the bottom of the trough, again centered by the confining walls. In order to maintain engagement of the actuator to the cube as shown in figure 10 to the end of the actuator travel, a semicircular slot is cut in the wall of the cube as detailed in figure 11. A total of 5 of these cuts will be needed; two on the "right" for "B" rotation, and three on the "left" for rotation type "C" to be discussed later.

Thus far we have followed the cube through three measurement steps (positions 1,2, and 5). From step three (position 5), shown approximately in figure 10(c), step four (position 6) is reached by engaging both actuators; step five (position 3) by another right actuator only, and step six (position 4) by a third activation of both L and R. Figure 12(a), (b) and (c) show the cube position for measurement steps four, five, and six.

After the measurement in step six is completed, the cube needs to be returned to the starting position (position 1) for tests at another parameter, such as a different frequency. This could be accomplished by a simple "B" rotation using actuator "R". However, this will give any cable attached to the cube a 360-degree twist. Activation of the "L" actuator three times in sequence will return the cube to the starting position without twisting the cable. The "L" actuator above produces a 90-degree turn about the same axis as a "B" rotation, but in the opposite direction. This is arbitrarily defined as a "C" rotation. Three "C" rotations (not shown in a figure) will return the cube to the starting position, as shown in figure 6. Table 2 summarizes the sequence of cube rotation types and the actuator-activation sequence. This sequence will need to be programmed on a controlling computer.

Table 2. Sequence of measurement steps, cube position changes, rotation types, and actuator sequencing for a complete cycle

STEP NUMBER	POSITION TRANSITION		CUBE ROTATION TYPE	ACTUATOR ACTIVATION
	From	To		
1	1	2	A	L R
2	2	5	B	R
3	5	6	A	L R
4	6	3	B	R
5	3	4	A	L R
6	unwinding		C	L
7	unwinding		C	L
8	return to 1		C	L

There are devices designed to be self-contained and battery-operated, including a spherical-dipole radiator used to verify this technique [7].

This class of radiators present few problems in performing this type of measurement. However the majority of devices that require characterization are not so simple. Most devices require interconnections to a larger system or, at a minimum, connection to a power source. Any metallic cables complicate measurements. Whenever possible these connections should be done with fiber-optic or high-resistance lines which have a minimal perturbation on the electromagnetic field.

Two significant issues to deal with in performing radiated measurements on devices and their associated cabling are defining what constitutes the DUT and controlling the effects of that part of the system external to the defined DUT. These issues and others are addressed in [1] for typical susceptibility measurements at a fixed orientation in the TEM cell. The DUT is carefully positioned in the TEM cell and the excess cable lengths are concealed using metal tape or removed from the cell as much as possible.

The multiple orientations of this technique, however, require that the DUT remain essentially the same for each position and the effect of the connecting cables also remain constant. The sequence of rotations outlined in table 2 makes it possible to handle equipment cables without tangling or twisting, to minimize the change in the nature of the DUT, and to control the effects of the cabling on the TEM field. By inserting the power or other instrumentation cable at the corner labeled "C" in figures 6, 7, 9, 10, and 12, the problem of cable handling is simplified. First, as can be discerned by studying these figures, the cable will be in one of only two possible positions while the cube is in any of its six measurement positions. Figure 13 shows these two positions. It also shows the approximate electric-field and magnetic-field lines present in a TEM cell with a square cross section. A wide rectangular cross section would provide a more uniform field in the test region at the center of each half-space and a lower concentration of the field in the septum to sidewall gap region. If it were possible to always align the interconnecting cables to cross the

electric-field lines perpendicularly, the effects on the TEM field would be minimized. No matter where the cabling exits the TEM cell, it must cross the same potential difference, so the choice is only how the exposure is distributed along the length of cable. In general, the cables are going to have an effect on the TEM field and also on the definition of the DUT. To the extent that these effects can be estimated, they should be accounted for when calculating the source parameters or at least brought into the error estimations as detailed in [9]. Figure 13 shows a suggested contour for each of the two positions of the cable during measurement.

The details of the mechanical actuators used in the prototype construction to lift the two pawls have been left out. In practice, a third actuator to raise a "catcher bar" located in the center of the trough between slots "L" and "R" is desirable to prevent the cube from experiencing sudden accelerations during descent.

Completion-of-motion feedback to a controlling computer can be provided by a fiber-optic light path that is either interrupted or completed when the cube has settled into measurement position. More elegant feedback that identifies the status of the possible positions can be implemented with three fiber-optic loops and appropriate binary coding applied to the eight cube edges that appear in the trough bottom through the complete cycle.

4. Electrical Measurements

The instrumentation requirements for this measurement may be grouped according to three test requisites. The first type of test is a complete characterization of the DUT at a single frequency including both radiation pattern and total power radiated. The second and less demanding test is where the total power radiated is desired but the radiation pattern is not.

This requires only amplitude measurements and is a subset of the first test type. The third test requirement relates to those DUTs which have a wide spectrum of emissions (i.e. digital circuits) and a complete characterization at each frequency is not practical. In this case amplitude measurements are made using a spectrum analyzer.

The measurement system includes the TEM cell, a sum and difference device, a detection instrument such as a vector analyzer, power meters, or spectrum analyzer, and a computer. The interconnecting coaxial cables must be carefully matched for electrical length and the signal path completely calibrated for losses and phase shifts. The TEM cell and the sum and difference device are selected based upon the frequency range of interest. In addition, the TEM cell must be large enough to accommodate the DUT. This will impose frequency constraints on the measurement [1]. A simple way to perform the sum and difference operation is with a 0° and 180° hybrid junction. These devices perform well and are available for frequencies above approximately two hundred kilohertz. When the desired frequencies fall below this or when the level of emissions is low and requires some amplification, the sum and difference function can be performed with an active circuit using operational amplifiers and other discrete components.

Figure 14 is a block diagram of a typical measurement system. A vector analyzer is required to measure the relative phase between the sum and difference ports, in addition to the amplitudes, for those tests requiring a complete characterization as noted in the first requirement above. The vector analyzer may be replaced with power meters or a coaxial switch and spectrum analyzer (for amplitude measurements only) if the radiation pattern is not desired. A word of caution in using the vector analyzer or power meters for devices that emit more than a single frequency signal is that the vector analyzer used in the tests presented in [7] and power meters in general do not discriminate against signals at frequencies other than the one under test and may give distorted results. These instruments should be

used with devices that exhibit single frequency emissions. When the test plan requires a complete characterization and the signal from the DUT contains multiple frequencies, it may be necessary to use a pre-selector or bandpass filter prior to the vector analyzer to select the desired frequency. A phase-amplitude receiver may be an alternative, if available in the desired frequency range.

The measurement becomes simpler when the phase requirement is removed. The sum and difference amplitudes may be measured by power meters or a spectrum analyzer. The power meters are less expensive and typically more accurate than a spectrum analyzer; however a power meter will respond to all frequencies present, and gives distorted results. There are some advantages to using a spectrum analyzer instead of power meters, such as increased dynamic range and the ability to distinguish specific frequencies. The spectrum analyzer may also be used to concurrently perform amplitude measurements at each of the many frequencies within the frequency-span setting of the instrument for a single series of mechanical rotations. This is essential for those devices containing a wide spectrum of emissions and very useful for any multiple-frequency device because the frequency-selection mechanism is contained in the spectrum analyzer.

The measurement sequence and data-analysis process are diagrammed in figure 15 to aid in development of a computer program designed to implement this technique. Figure 15 shows the various options for performing the measurement and processing the data that have been discussed.

5. Concluding Remarks

The TEM cell can be a powerful tool in the evaluation of electromagnetic properties of electrically small devices. The theoretical

basis for complete characterization of an unknown emitter has been developed earlier. This paper has explored some of the practical problems in the implementation of this measurement procedure. Suggestions to solutions for handling the interconnecting cables and automating the mechanical rotation process have been presented. This information along with the mathematical details in [7] and [9], and good measurement practice should enable this technique to be an efficient and useful tool for the study of radiated emissions from a wide variety of devices.

6. References

- [1] Crawford, M. L.; Workman, J. L. Using a TEM cell for EMC measurements of electronic equipment. NBS Tech Note 1013, July 1981.
- [2] Crawford M. L. Generation of standard EM fields using TEM transmission cells. IEEE Trans. EMC, vol. EMC-16, No. 4, pp. 189-195, Nov 1974.
- [3] Kanda, M.; Orr, R. D. Generation of standard electromagnetic fields in a TEM cell. NBS Tech Note 1319, July 1988.
- [4] Sreenivasiah, I.; Chang, D. C.; Ma, M. T. A method of determining the emission and susceptibility levels of electrically small objects using a TEM cell. NBS Tech Note 1040, April 1981.
- [5] Sreenivasiah, I.; Chang, D. C.; Ma, M. T. Characterization of electrically small radiating sources by tests inside a transmission line cell. NBS Tech Note 1017, Feb 1980.
- [6] Sreenivasiah, I.; Chang, D. C.; Ma, M. T. Emission characteristics of electrically small radiating sources from tests inside a TEM cell. IEEE Trans. EMC, vol. EMC-23, No. 3, pp. 113-121, Aug 1981.
- [7] Ma, M. T.; Koepke, G. H. A method to quantify the radiation characteristics of an unknown interference source. NBS Tech Note 1059, Oct 1982.

- [8] Collin, R. E. Field Theory of Guided Waves, New York, McGraw-Hill Book Company, 1960.
- [9] Ma, M. T.; Koepke, G. H. Uncertainties in extracting radiation parameters for an unknown interference source based on power and phase measurements. NBS Tech Note 1064, June 1983.

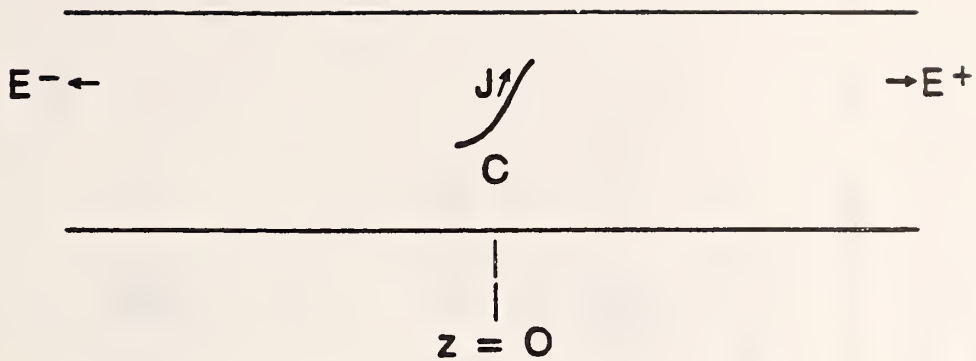


Figure 1. An arbitrary current source inside one half of a TEM cell.

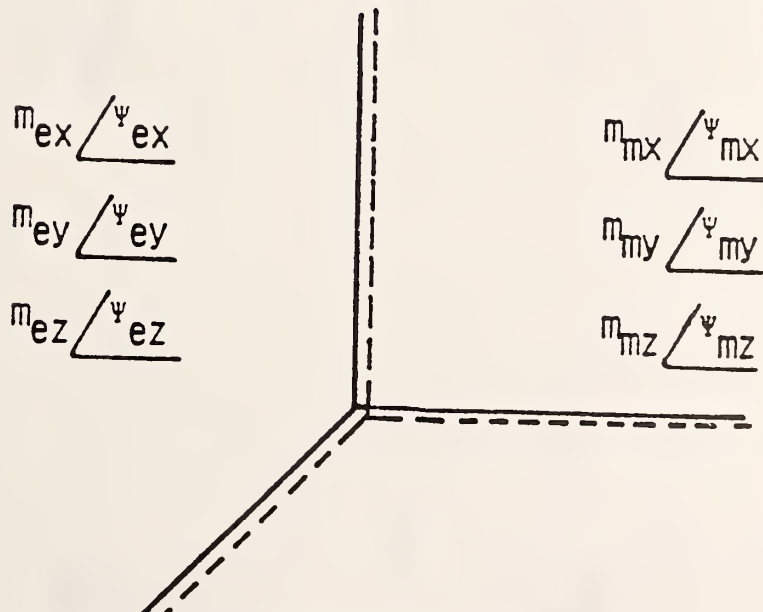
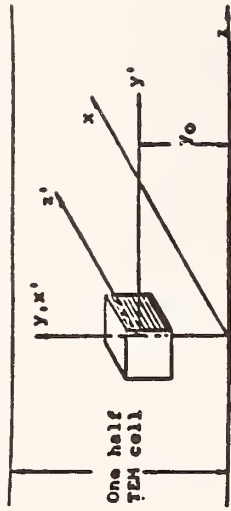
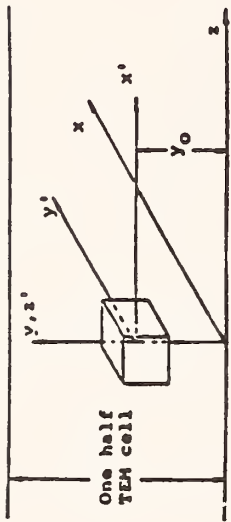


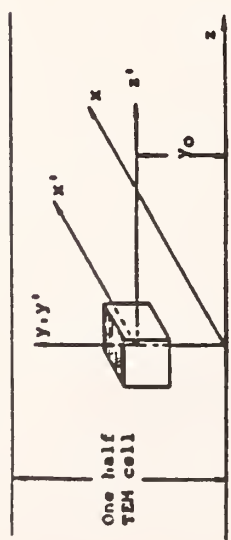
Figure 2. The device under test (DUT) is modeled by three equivalent orthogonal electric and three equivalent orthogonal magnetic dipoles.



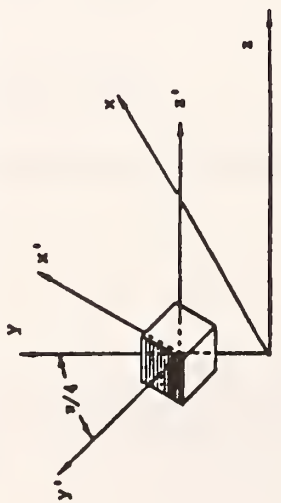
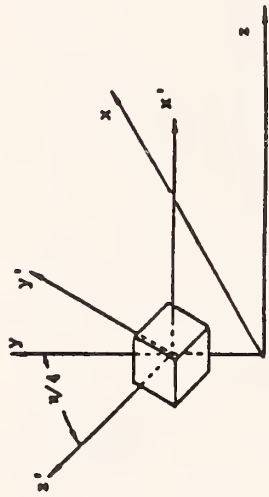
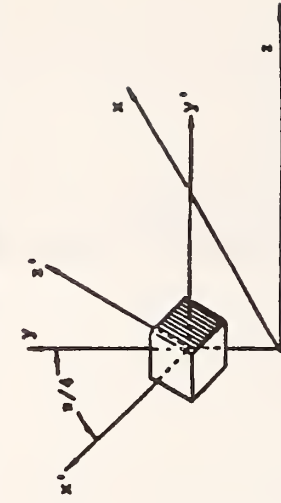
Preliminary alignment for 5 and 6



Preliminary alignment for 3 and 4



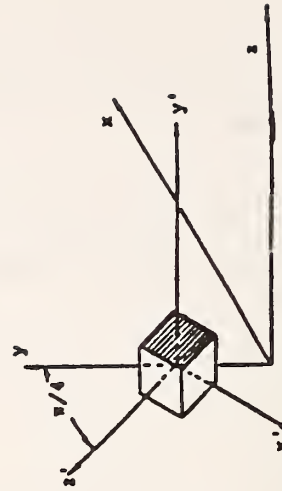
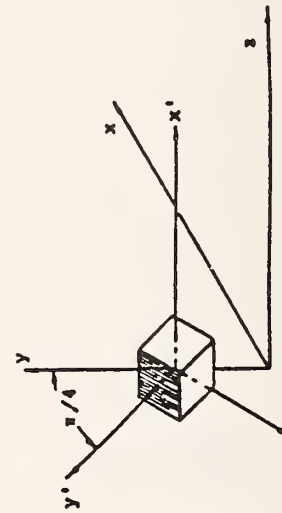
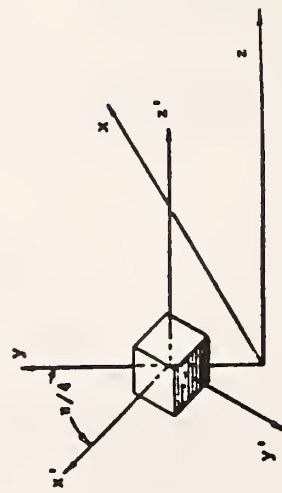
Preliminary alignment for 1 and 2



Position 1

Position 3

Position 5



Position 2

Position 4

Position 6

Figure 3. The six required orientations of the DUT inside a TEM cell.

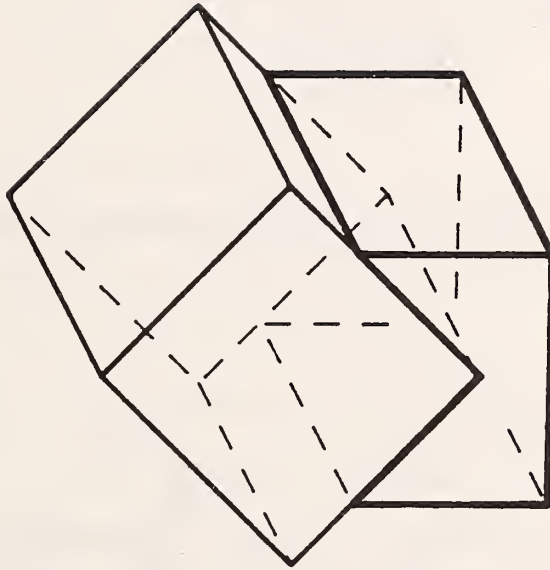
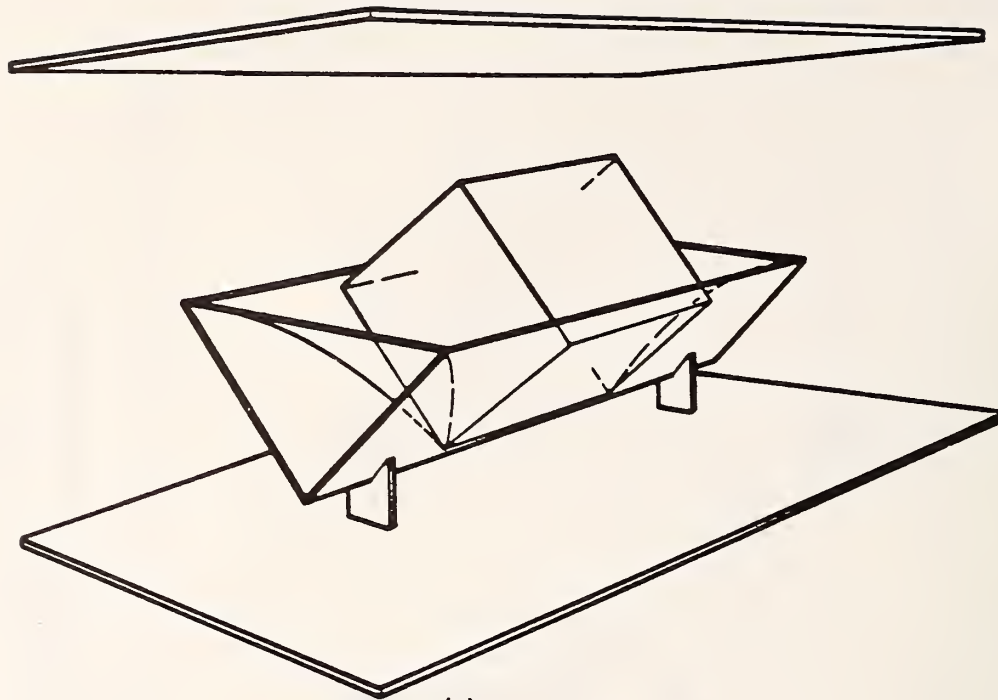
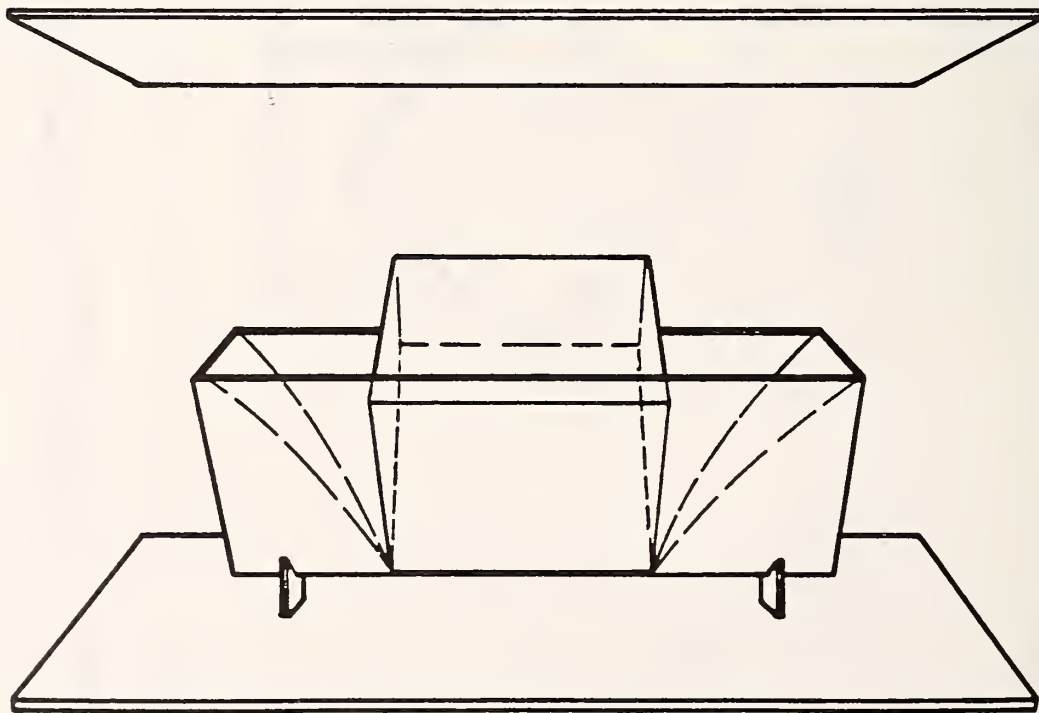


Figure 4. A simple dielectric cube and trough for positioning the DUT inside the TEM cell. The DUT is mounted inside the cube.



(a)



(b)

Figure 5. Two views of the dielectric positioner for use inside a TEM cell.

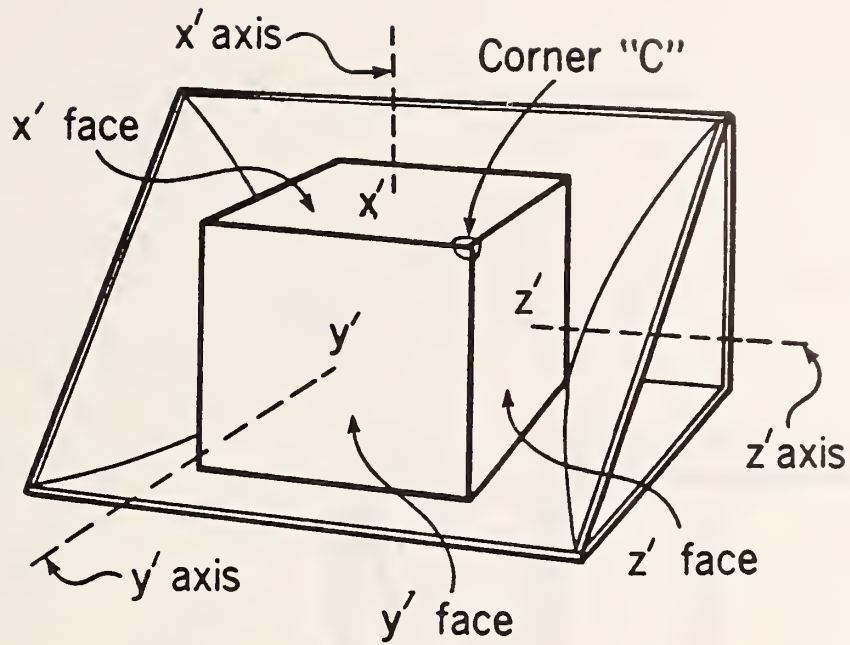


Figure 6. The face and axis definitions of the cube at the initial position.

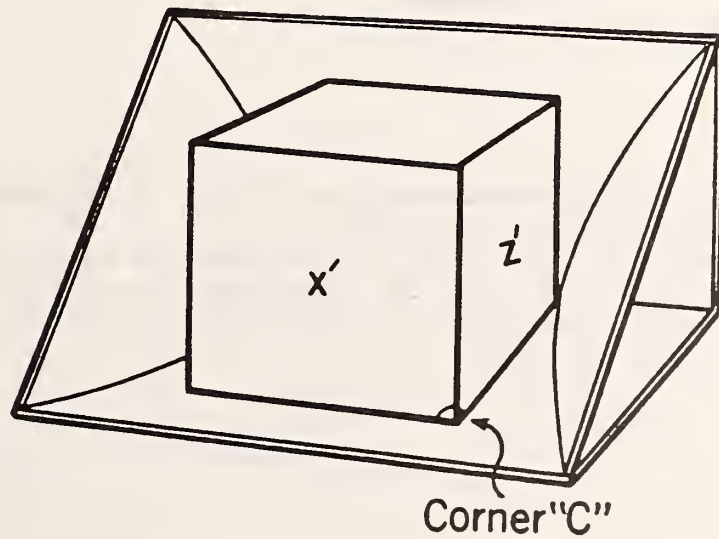


Figure 7. The cube position at the second measurement step.

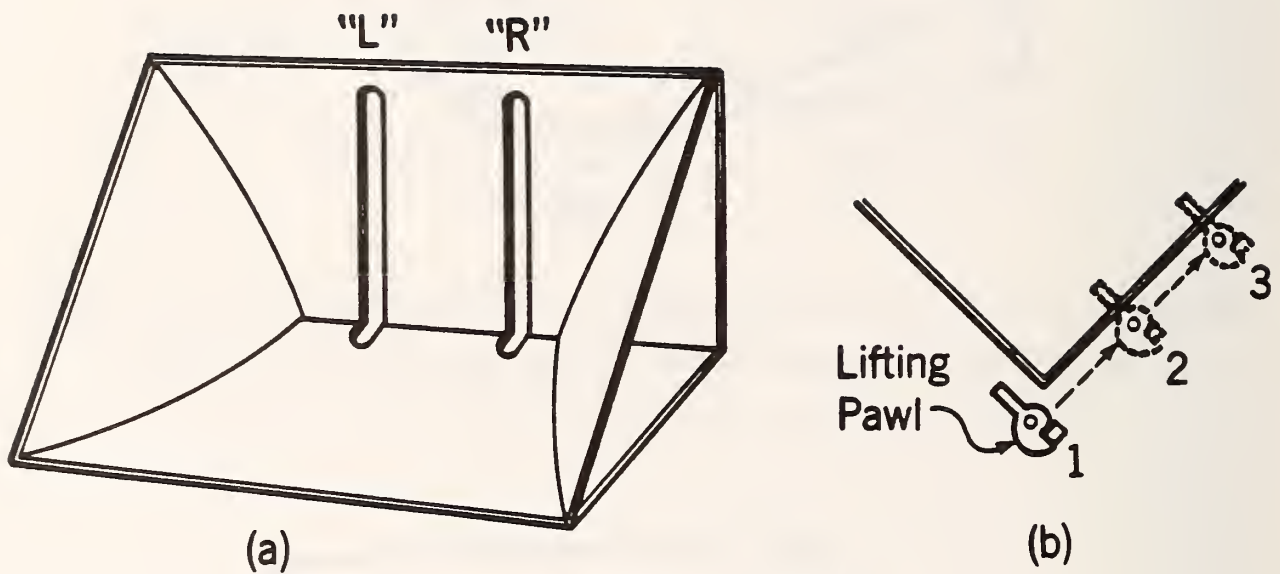


Figure 8. (a) Schematic representation of the 2 slots in the back wall of the trough, "L" (left) and "R" (right).
(b) The view along the trough axis showing the schematic of a lifting pawl within a slot. The three positions, initial (1), intermediate (2), and final (3) are shown for each of the pawls moving in slots "L" and "R".

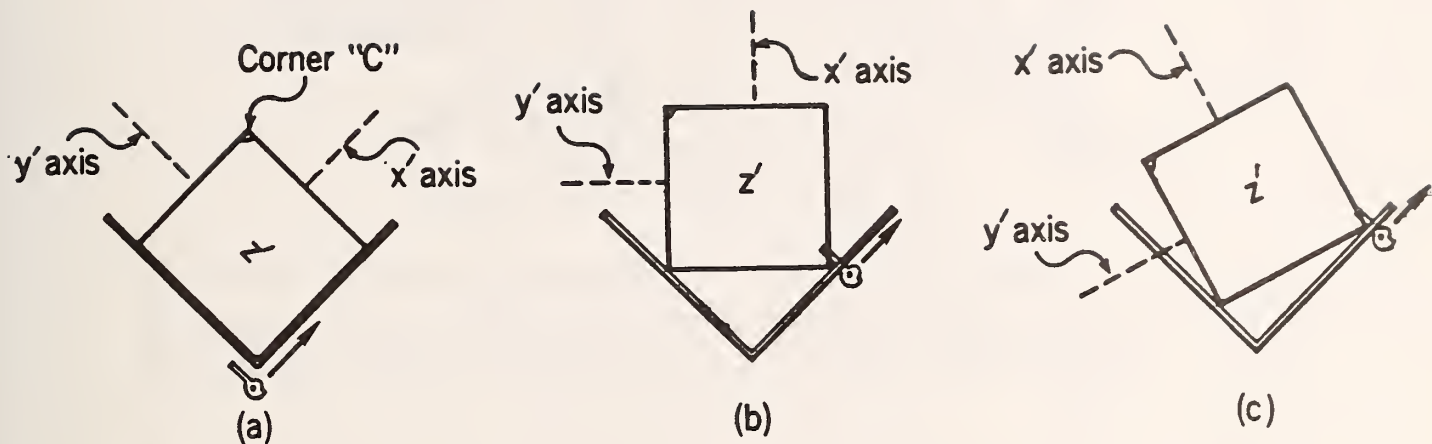


Figure 9. Cube rotation, from the initial to the second measurement step, caused by the three successively higher positions of both the "L" and "R" lifting pawl actuators. This is defined as an "A" rotation, which is 90° .

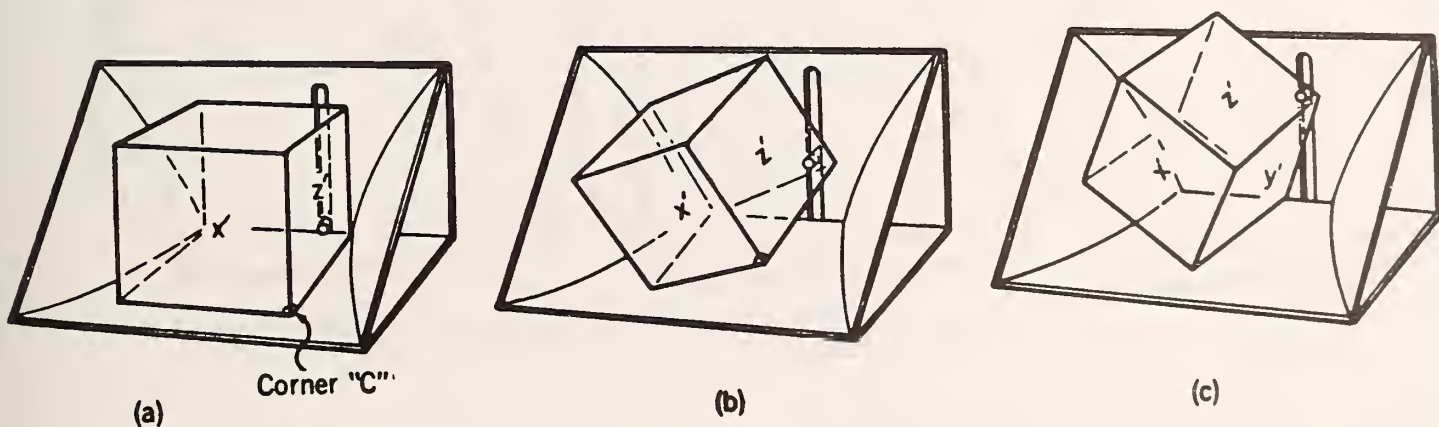


Figure 10. Cube rotation, from the second to the third measurement positions, caused by the three successively higher positions of only the "R" actuator pawl. This is defined as a "B" rotation, which is 90° . The "L" actuator, and left slot are omitted for clarity.

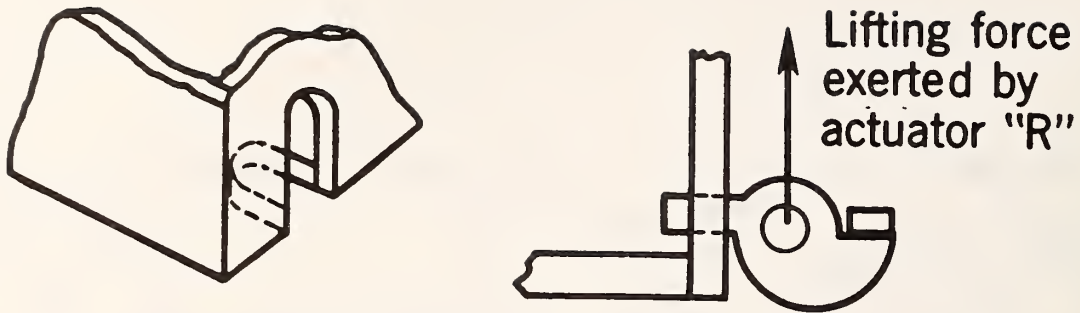


Figure 11. Detail of one of the two slots cut in the cube wall to engage the "R" lifting pawl needed for single actuator rotators (type B) of the cube.

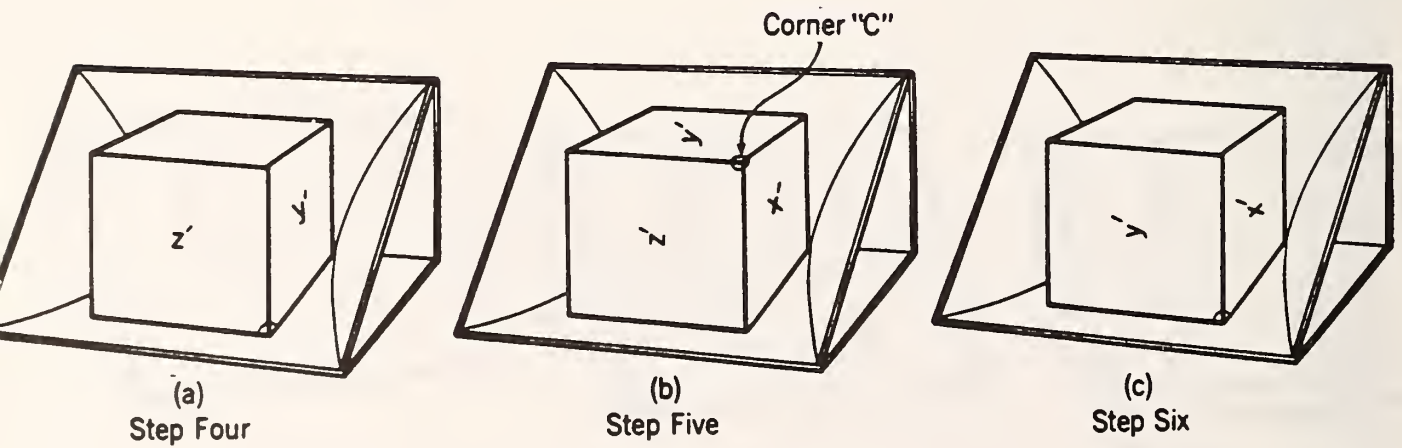


Figure 12. Cube positions for measurement step numbers four, five, and six.

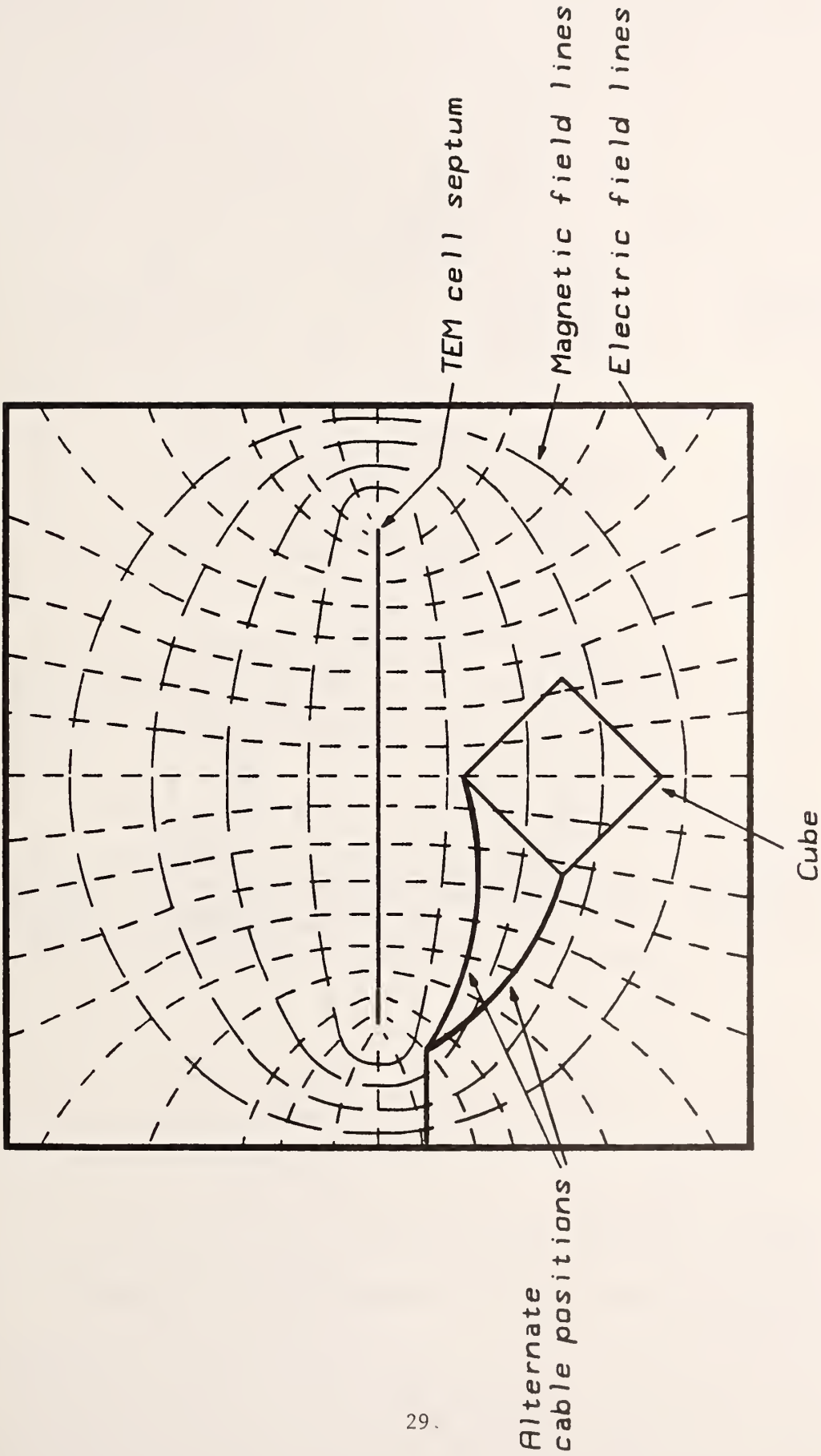


Figure 13. Cross-sectional view of a TEM cell showing the two cable positions which occur as the cable rotates. Also shown are the approximate electric and magnetic field lines in the cell.

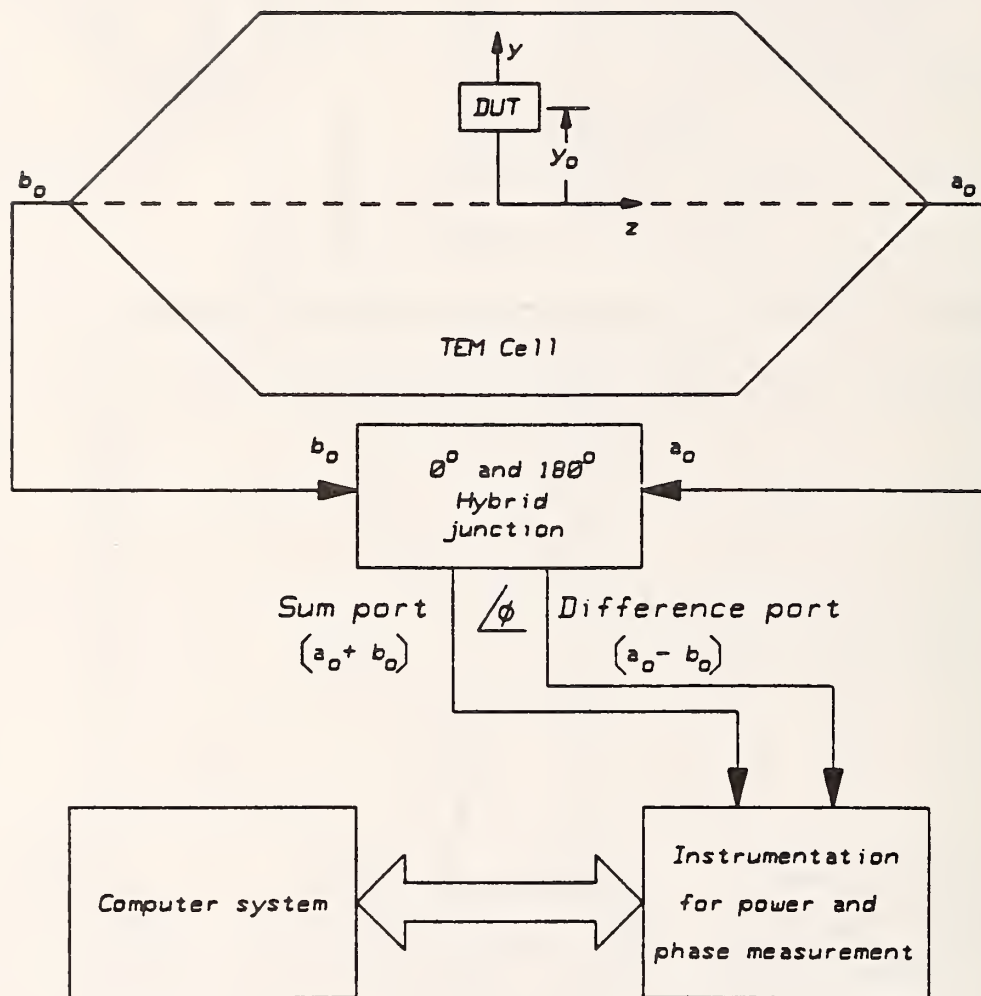


Figure 14. Radiated emissions testing measurement system.

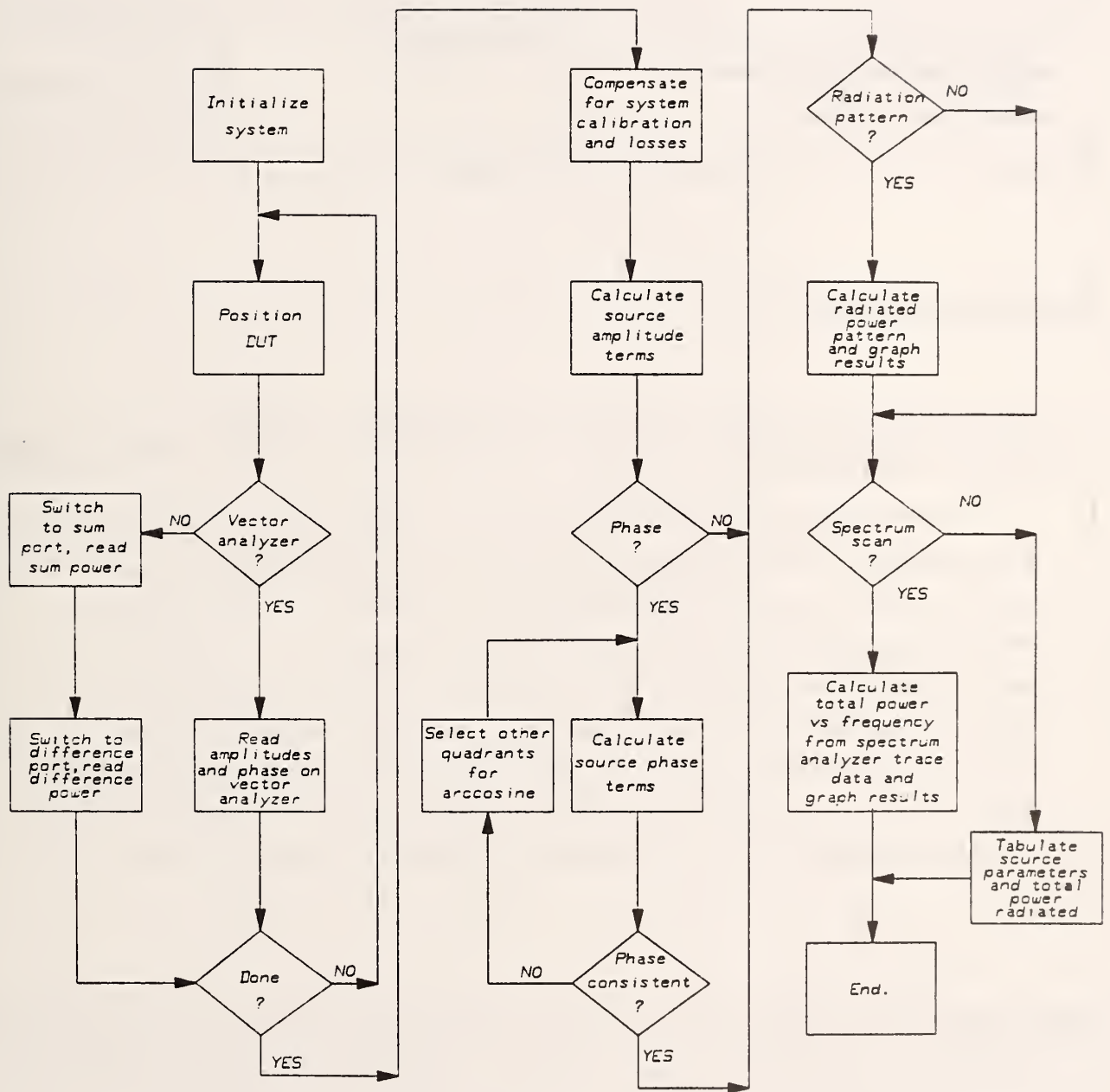
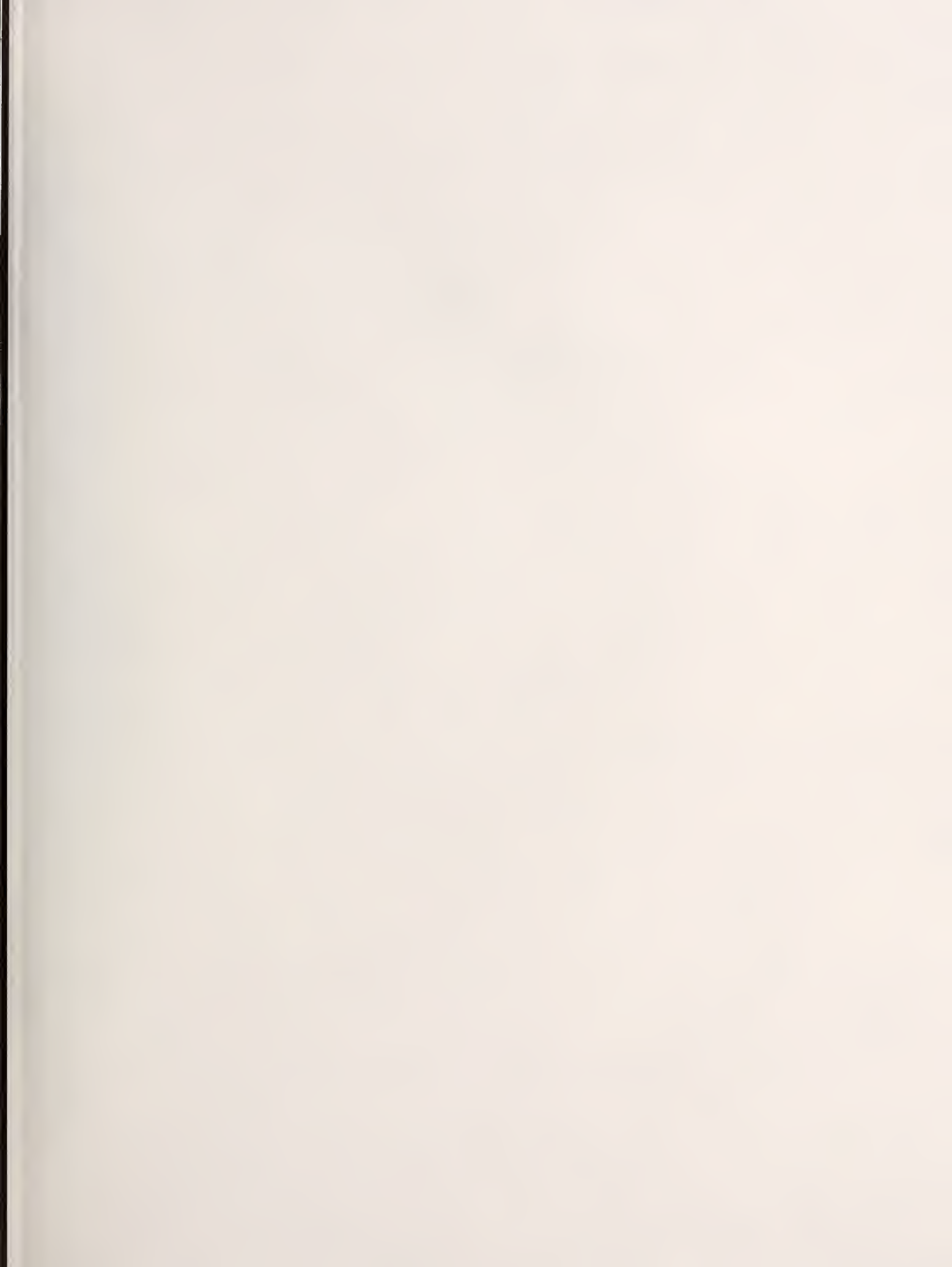


Figure 15. A flow diagram of the measurement and analysis sequences.

U.S. DEPT. OF COMM. BIBLIOGRAPHIC DATA SHEET (See instructions)	1. PUBLICATION OR REPORT NO. NIST/TN-1326	2. Performing Organ. Report No.	3. Publication Date January 1989
4. TITLE AND SUBTITLE Theory and Measurements of Radiated Emissions Using a TEM Cell			
5. AUTHOR(S) G.H. Koepke, M.T. Ma, and W.D. Bensema			
6. PERFORMING ORGANIZATION (If joint or other than NBS, see instructions) National Institute of Standards and Technology NATIONAL BUREAU OF STANDARDS DEPARTMENT OF COMMERCE WASHINGTON, D.C. 20234		7. Contract/Grant No.	8. Type of Report & Period Covered
9. SPONSORING ORGANIZATION NAME AND COMPLETE ADDRESS (Street, City, State, ZIP)			
10. SUPPLEMENTARY NOTES <input type="checkbox"/> Document describes a computer program; SF-185, FIPS Software Summary, is attached.			
11. ABSTRACT (A 200-word or less factual summary of most significant information. If document includes a significant bibliography or literature survey, mention it here) <p>The transverse electromagnetic cell is widely used to evaluate the electromagnetic characteristics of electrically small devices. This paper reviews the theoretical basis for a technique to quantify the radiated emissions from any such device in the cell. The technique is well suited to an automated test system provided that the mechanical motions required can be controlled by a computer. The difficulties associated with these mechanical motions are discussed and possible solutions are proposed. The measurement technique is also expanded to include multiple-frequency sources in addition to single-frequency sources.</p>			
12. KEY WORDS (Six to twelve entries; alphabetical order; capitalize only proper names; and separate key words by semicolons) automation; electrically small radiator; emissions; measurements; TEM cell			
13. AVAILABILITY <input checked="" type="checkbox"/> Unlimited <input type="checkbox"/> For Official Distribution. Do Not Release to NTIS <input checked="" type="checkbox"/> Order From Superintendent of Documents, U.S. Government Printing Office, Washington, D.C. 20402. <input type="checkbox"/> Order From National Technical Information Service (NTIS), Springfield, VA. 22161		14. NO. OF PRINTED PAGES 40	15. Price



U.S. DEPARTMENT OF COMMERCE
National Institute of Standards and Technology
(formerly National Bureau of Standards)
325 Broadway
Boulder, Colorado 80303-3328

OFFICIAL BUSINESS
PENALTY FOR PRIVATE USE \$300